Modeling Maximum Hail Size in Alberta Thunderstorms

JULIAN C. BRIMELOW AND GERHARD W. REUTER

Department of Earth and Atmospheric Sciences, University of Alberta, Edmonton, Alberta, Canada

EUGENE R. POOLMAN

South African Weather Service, Pretoria, South Africa

(Manuscript received 7 September 2001, in final form 20 May 2002)

ABSTRACT

A one-dimensional steady-state cloud model was combined with a time-dependent hail growth model to predict the maximum hailstone size on the ground. Model runs were based on 160 proximity soundings recorded within the Alberta Hail Project area for three summers between 1983 and 1985. The forecast hail sizes were verified against reports of maximum hail size gathered from a high-density observation network within the project area. The probability of detection (POD), the false-alarm ratio (FAR), and the Heidke skill score (HSS) were computed for the hail model forecasts and were compared with the skill scores for a nomogram method developed to forecast hail size in Alberta. The hail model was skillful in forecasting hail (POD = 0.85, FAR = 0.26, HSS = 0.64). On days with hail larger than 2 cm in diameter, the hail model performed slightly better (POD = 0.90, FAR = 0.40, HSS = 0.67). Analysis of the skill scores and hail-size forecasts suggests that employing a coupled cloud and hail model noticeably improves the overall skill and accuracy of hail forecasts as compared with those determined using the nomogram.

1. Introduction

Hailstorms occur frequently over central Alberta during the summer months, with hail observed on an average of 51 days between 1 June and 31 August (Smith et al. 1998). On average, there are about 20 days per summer with severe hail (hailstone diameter greater than 2 cm). Strong and Lozowski (1977) found that hail damage to crops increased logarithmically with increasing kinetic energy of the hailstones. This strong dependence on hail size is related to the fact that for a spherical hailstone of diameter d the kinetic energy is roughly proportional to d^4. Thus, to forecast the damage potential of hail, it is important to predict the maximum size of the hailstones. However, despite significant advances in our understanding of severe thunderstorms, the short-range forecasting of hail size remains challenging.

Weather radar is widely employed to monitor the structure, severity, and development of thunderstorms. For example, dual-polarization radar techniques have been used to identify the presence hail in thunderstorms (Al-Jumily et al. 1991). Radar-derived parameters, such as the vertically integrated liquid (VIL) and the hail detection algorithm of Witt et al. (1998), are also often used to detect and to nowcast hail. However, Edwards and Thompson (1998) found that VIL-based parameters currently used to predict hail severity show limited skill. Moreover, Witt et al. (1998) noted that predicting maximum hail diameter was the most challenging aspect of their hail detection algorithm. The most significant caveat of current radar-derived hail algorithms is that they only indicate hail after it has commenced or that it is imminent. Thus, little or no lead time can normally be achieved when issuing and disseminating severe-weather warnings.

To identify the likelihood of hail prior to the formation of thunderstorms, one might consider hail forecasting techniques based on prestorm atmospheric sounding data. Fawbush and Miller (1953) made one of the earliest attempts to forecast hail size (on the ground) using observed rawinsonde soundings of temperature, dewpoint, and wind. They developed a nomogram that related the maximum expected hail size on the ground to the positive buoyant energy between the cloud base and level of the −5°C isotherm. Their nomogram technique has been of limited use, however. For example, Leftwich (1984) evaluated Fawbush and Miller's technique and calculated a root-mean-square error of 2.5 cm for the forecast hail size. Foster and Bates (1956) adopted a similar approach to that of Fawbush and Miller but related the maximum expected hail size to the updraft velocity at −10°C. Verification of Foster and Bates's

Corresponding author address: Gerhard Reuter, Dept. of Earth and Atmospheric Sciences, University of Alberta, Edmonton, AB T6G 2E3, Canada.
E-mail: gerhard.reuter@ualberta.ca

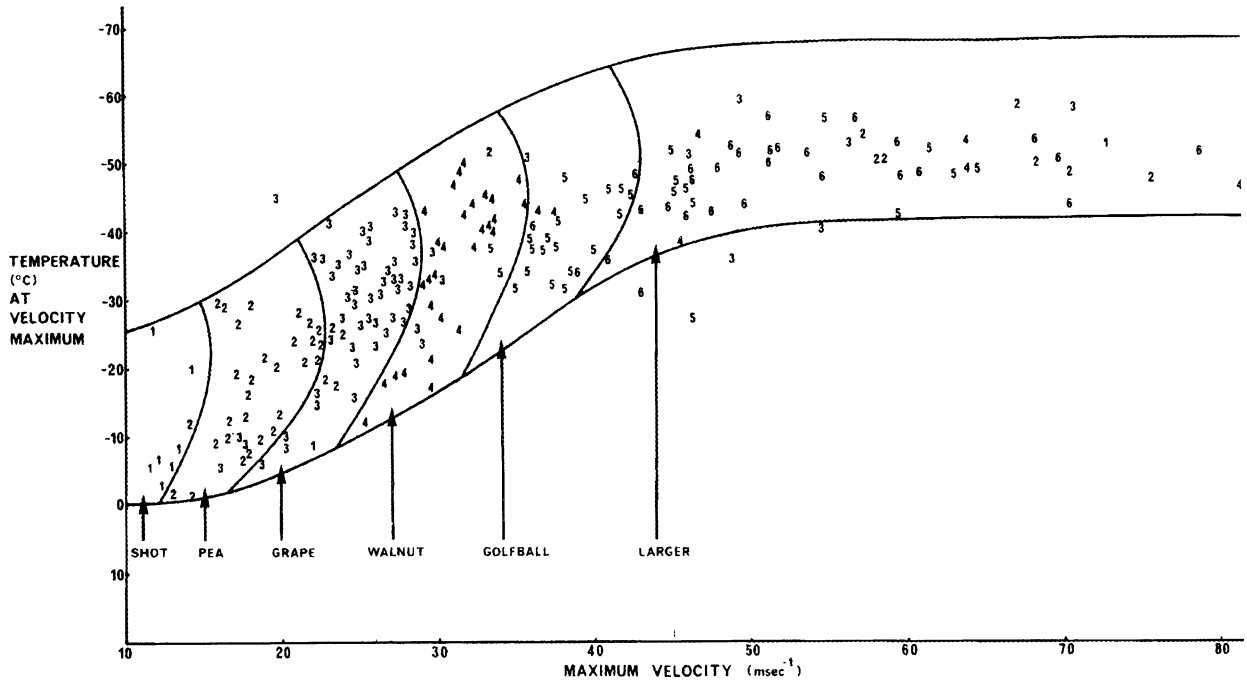

FIG. 1. Nomogram developed by Renick and Maxwell (1977) that relates the maximum observed hail size on the ground to the forecast maximum updraft velocity and the temperature at the updraft maximum. Numbers 1–6 correspond to shot- through greater-than-golfball-size hail. Adapted from Renick and Maxwell (1977).

approach revealed that it often failed to discriminate between large and small hail events (Doswell et al. 1982).

Renick and Maxwell (1977) developed a nomogram that related the hail size on the ground to the maximum updraft velocity and temperature at the updraft maximum (Fig. 1). They used Chisholm's (1973) one-dimensional steady-state cloud model to conduct diagnostic model runs for 210 hail days between 1969 and 1973 for the Alberta Hail Project. The forecast maximum updraft velocity and the temperature at the height of the updraft maximum showed the highest correlation with the maximum observed hail size. Hail-size forecasts based on their nomogram require minimal computing time and avoid the complications of modeling the growth and melting of hail. Moore and Pino (1990) adopted Foster and Bates's approach but calculated the vertical velocity using the one-dimensional steady-state cloud model of Anthes (1977). Their method relates the hail diameter to the vertical velocity (based on a modified sounding) at -10°C and allows for the effect of melting on the hailstone's size before reaching the ground. They found the skill of their model to be far superior to that of Fawbush and Miller for 58 severe hail events over the southern plains of the United States. Moore and Pino's technique has yet to be evaluated for no-hail and nonsevere hail days.

Multidimensional, time-dependent hail models have been widely used to simulate hailstorms and have contributed to our current understanding of hail growth mechanisms (e.g., Orville and Kopp 1977; Clark 1982; Xu 1983; Farley 1987; Kubesh et al. 1988). However, these models require extensive computing resources. Brooks et al. (1992) discussed the formidable challenges involving initialization of three-dimensional (3D) cloud models. Furthermore, field experiments using 3D cloud models are limited to relatively small areas, and access to the model's output is only available to a select group of clients (Brooks et al. 1993). To avoid these shortcomings, Dennis and Musil (1973) employed a simple one-dimensional (1D) model. A major difficulty with that approach, however, is to simulate realistically the evolutionary aspects of deep convection.

This paper will address the problem of predicting maximum hail size on the ground using a one-dimensional steady-state cloud model coupled with a time-dependent hail growth model. This approach is used operationally by the South African Weather Service to forecast hail size (Poolman 1992). The model has also been further developed to improve some of the hail microphysics and the coupling of the time-dependent and steady model components (Brimelow 1999). However, the model has not undergone a detailed evaluation because of the lack of systematic hail observations in South Africa. The main difficulty in evaluating model hail forecasts lies in the high temporal and spatial variability of the hailfall. Morgan and Towery (1975) analyzed a hailstorm that moved over a high-density observation network with hail pads spaced about every 200 m. Maximum sizes ranged from 1 to 3 cm. The

largest hail (3 cm) covered only 1% of the total area of the network; 80% was covered by hail smaller than 2 cm in diameter. Therefore, a coarse observation network would very likely have underestimated the maximum hail size produced by this storm. Also, when evaluating the skill of a cloud and hail model, it is imperative to use sounding and surface data representative of the environmental conditions in which the thunderstorms develop. Obtaining proximity soundings is complicated by the high spatial and temporal variability typically evident in a thunderstorm environment. Proximity soundings are usually identified by applying spatial and temporal constraints between the soundings and the observed storms. For example, Brooks et al. (1994) selected proximity soundings by identifying all soundings within 160 km and 1 h of storm observations. Soundings satisfying these constraints were then inspected subjectively to identify and to remove problem soundings (i.e., convectively contaminated or unrepresentative soundings). Moore and Pino (1990) used hail events that occurred within 3 h of the sounding time and 100 km of the launch site to evaluate their hail forecasting technique.

The objective evaluation of model-derived hail forecasts is thus contingent on two criteria: an extended period of accurate hail reports from a high-density observation network and sounding and surface data representative of the environmental conditions in which the thunderstorms develop. This investigation aims to satisfy these criteria by drawing on the comprehensive dataset archived during the Alberta Hail Project (AHP) to evaluate the model forecasts. The AHP is considered to be one of the longest-running and best-documented hail observation networks in the world (Admirat et al. 1985).

In section 2, we provide details of the AHP dataset used to evaluate the hail forecasts. Section 3 provides a description of the model components and addresses the complexities of coupling a time-dependent hailstone growth model with a steady-state 1D cumulus model. In section 4, an example of the model-derived updraft profile and hail growth history for a severe hail day is presented. This section also contains the sensitivity analysis of the modeled cloud and hail growth to various input parameters. We also determine whether utilizing a time-dependent hail growth model can improve the accuracy of the hail-size forecasts over those made using the nomogram of Renick and Maxwell (1977). In section 5, forecasts of maximum hail size determined using the model and the nomogram are evaluated against hail observations from the AHP for three summers between 1983 and 1985. Section 6 identifies the shortcomings of the forecast techniques, and we conclude with a summary and suggestions for future research in section 7.

2. Observations

The Alberta Hail Project was an intensive field study of Alberta hailstorms and lasted from 1957 to 1985 (Admirat et al. 1985; Smith et al. 1998). The project area covered 33 700 km^2 and was centered on the Penhold radar site located at 52.2°N, 113.9°W (Smith and Yau 1993a). Its dual purpose was to conduct research on hailstorms and to assess the potential of reducing hail damage through cloud seeding (Deibert 1984). Each spring, hail cards were mailed to approximately 20 000 farmers in the project area. On days with hail, between 10% and 20% of the farmers responded, yielding an average of one observer per 16–32 km^2 (Smith et al. 1998). In addition to the hail-card reports, telephone surveys were also conducted on days with hailstorms, resulting in observation densities as high as one report per 3 square kilometers. As a result, it is believed that only a very small percentage of hail reaching the surface went undetected.

Observers within the AHP were requested to report the largest and most common hail sizes. For the duration of the project, six categories were specified to size the observed hailstones conveniently: shot, diameter less than 0.4 cm; pea, 0.4–1.2 cm; grape, 1.3–2.0 cm; walnut, 2.1–3.2 cm; golfball, 3.3–5.2 cm; and larger than golfball, larger than 5.2 cm (Strong 1974). Comparisons with measurements using aluminum hailpads indicated that the observed hail sizes had an error margin of approximately 10% (Admirat et al. 1985).

To capture the atmospheric conditions during thunderstorm outbreaks, upper-air soundings were released from Penhold at 1715 local time (LT). Data were only used for the model evaluation if hail was reported within 3 h (i.e., between 1415 and 2015 LT) and within 100 km from the sounding site. These criteria for selecting proximity soundings are similar to those used by Leftwich (1984), Moore and Pino (1990), and Brooks et al. (1994). A few of these proximity soundings had to be excluded because of missing data or because they were modified by precipitation or a thunderstorm outflow boundary. The model evaluation was confined to three summer periods (20 June–30 August) in 1983, 1984, and 1985. During these periods, telephone surveys of hail size were conducted in addition to the hail network observations.

A total of 219 soundings were screened, and 160 of these (73% of the available soundings) were identified as proximity soundings. Of the 160 soundings used in our investigation, 98 (61%) were made on days with no hail, 42 (26.5%) were made on days with hail smaller than walnut, and 20 (12.5%) were made on days with walnut or larger hail (diameter greater than 2.0 cm). Although there is no way of unequivocally determining whether the soundings adequately depicted the storm-scale setting on all days, we believe our selection criteria yielded representative soundings given the temporal and spatial limitations of the Penhold sounding dataset. In addition to upper-air sounding data, the cloud model requires the surface temperature and dewpoint that represent the surface air feeding the core updraft of the storm. To do this, the soundings were modified using

the surface temperature and dewpoint (representative of the storm's inflow) obtained from a mesonetwork.

3. Model description

Our approach for predicting the maximum hail size is to couple a time-dependent hail growth model with a one-dimensional steady-state cloud model. This combined model (hereinafter referred to as ''HAILCAST'') has been documented by Poolman (1992) and Brimelow (1999), and here only a brief overview is provided.

a. The hail model

The governing equations of the time-dependent hail growth model are those used by Musil (1970), Dennis and Musil (1973), and Rasmussen and Heymsfield (1987a,b). A hail embryo is placed within an updraft where it accretes supercooled cloud water droplets and ice crystals. The rate of accretion is determined by the mass and heat budgets of the hailstone, which depend on the hailstone's size and the in-cloud conditions (such as updraft velocity, temperature, and cloud liquid water content). The hail growth calculations are based on the assumption that the modeled hailstone is spherical and that the temperature is uniform throughout the hailstone. It is also assumed that the accreted water and ice form a high-density (0.9 g cm^{-3}) deposit. Low-density ice growth is possible at low temperatures and low liquid water contents, and the resulting change in the stone's terminal velocity can alter the trajectory and growth of the stone (e.g., Ziegler et al. 1983). However, because the majority of hailstones collected in the field have a density close to 0.9 g cm^{-3} (Macklin 1977), it probably is adequate to allow only high-density growth.

The growth of hail is initiated by introducing a 300-μm-diameter droplet at the cloud base. This droplet acts as a hail embryo and is assumed to originate from the shedding of water from the surface of melting hail already present in the cloud (Rasmussen and Heymsfield 1987c). The droplet is assumed to freeze as it passes through the -8°C level. Above the -20°C level, it grows by intercepting supercooled water droplets and cloud ice. The amount of cloud ice is determined using the relation proposed by Vali and Stansbury (1965), which depletes the cloud water exponentially from near-adiabatic values at -20°C to zero at -40°C. After each time step, the hydrometeor is advected to a new height that depends on the difference between its terminal fall speed and the updraft velocity. The surface temperature and change in mass (and new diameter) are then calculated at the new height. Also, depending on the heat transfer to and from the hailstone, it enters the wet or dry growth regime. The ventilation coefficient used in the heat balance equations is calculated according to the method of Rasmussen and Heymsfield (1987a). In the wet growth regime, excess water is shed if the mass of water present on the hailstone's surface exceeds a critical limit determined using the empirically derived linear relationship of Rasmussen and Heymsfield (1987a). In the dry growth regime, all the accreted water is frozen. The hailstone continues to grow until its fall speed exceeds that of the updraft or the updraft collapses. No more growth occurs below the freezing level because of the shedding of meltwater from the hailstone's surface.

b. The cloud model

The one-dimensional steady-state cloud model of HAILCAST is very similar to the models developed by Simpson and Wiggert (1969), Chisholm (1973), Sanders and Garett (1975), Matthews and Henz (1975), and Anthes (1977).

When modeling the vertical velocity and saturation mixing ratio profiles in convective clouds, it is important to account for the effect of entrainment on the updraft. As a cumulus tower grows, drier environmental air is entrained through the cloud's top (cloud-top entrainment) and sides (lateral entrainment). The mixing of the relatively cool and dry environmental air with the updraft lowers the saturation mixing ratio and temperature of the updraft air, thereby decreasing its buoyancy. Clouds with weaker updrafts tend to experience more entrainment, and clouds with strong updrafts typically have a moist-adiabatic core (Paluch 1979; Bluestein et al. 1988). Boatman and Auer (1983) and Blyth et al. (1988) showed that cloud-top entrainment dominates in large cumulus clouds. Updrafts in smaller cumulus clouds are diluted mainly by lateral entrainment (Blyth et al. 1988). Poolman's cloud model parameterizes both cloud-top and lateral entrainment using the saturation-point analysis scheme of Betts (1982a,b). Betts's saturation-point analysis scheme allows the modeler to vary the percentage of environmental air that mixes with the in-cloud air. To avoid overly suppressing convection in our model runs, we did not allow Betts's entrainment parameter β to exceed 0.10. In other words, no more than 10% of the condensed water is allowed to evaporate as the parcel rises. Once the effect of entrainment on the parcel's temperature and saturation mixing ratio has been taken into account, the updraft velocity W is calculated as follows:

$$W^2 = W_0^2 + 2g \int_{z_{lcl}}^{z_{el}} \left(\frac{T^* - T}{T} - \chi \right) dz,$$

where W_0 is the updraft velocity at the lifting condensation level, g is the gravitational acceleration, z_{lcl} is the lifted condensation level, z_{el} is equilibrium level, and T^* and T are the virtual in-cloud and ambient temperatures, respectively. We assume $W_0 = 4$ m s^{-1}, based on Chisholm's (1973) measurements of cloud-base updraft velocities in Alberta hailstorms. The water-loading term χ represents the mixing ratio of condensed water substance present at each level within the cloud after

entrainment. The model does not explicitly include nonhydrostatic pressure perturbation effects.

An upper-air sounding (a vertical profile of temperature, moisture, and wind data) and the representative surface temperature and coincident dewpoint were used as input for the cloud model. For each sounding, the lifting condensation level (LCL) was determined by lifting the surface parcel adiabatically until saturation was achieved. On some days in the dataset, a very shallow layer of moisture was present near the surface. This ''skin layer'' of moisture was marked by a rapid decrease in dewpoint (>2°C) between the surface and the first data level at 900 hPa (50–150 m above the surface). If the difference in dewpoint between these two levels was greater than 2°C, then the dewpoint at 900 hPa was deemed more representative of the low-level moisture, and this value was used in the model simulations. HAILCAST is very computationally efficient, with a 60-min simulation taking less than 5 s on a 333-MHz personal computer.

Although the majority of severe thunderstorms is surface based (Rennó and Williams 1995), we recognize that elevated thunderstorms can occasionally produce severe hail (Colman 1990a,b). Severe elevated thunderstorms are rare in central Alberta, and we are confident that our assumption of surface-based convection is appropriate for the majority of hail days in this region. However, allowing for elevated convection may be important elsewhere in North America during the winter and spring months, when the frequency of elevated thunderstorms is greatest (Colman 1990a).

c. Coupling the cloud and hail model

Our model approach combines a steady-state cloud model with a time-dependent hail growth model. Although the model cloud conditions remain unchanged for an infinite time, the hailstone develops in a relatively short period. In fact, the residence time of a hailstone within the supercooled region of the cloud is a major factor controlling the stone's size (Nelson 1983; Miller et al. 1988). Therefore, for some storm clouds, it becomes necessary to limit the duration of the steady-state cloud conditions. Dennis and Musil (1973) addressed the problem of a steady-state updraft in their 1D model by generating time-dependent updraft profiles through a series of Fourier harmonics. To be specific, the Fourier series were determined by parameters such as the cloud lifetime (fixed at 60 min), cloud-top height, and the peak amplitude of the first and second harmonic, respectively. Their approach is feasible for conducting diagnostic case studies but is not well suited for an operational setting. Moreover, assuming a fixed storm lifetime of 60 min is not always appropriate, and there are no objective criteria for selecting the magnitudes of the amplitudes of the oscillations.

To introduce the rationale of our model coupling approach, we have to review some considerations of timescales appropriate for convection and hail growth, respectively. Foote (1984) identifies the timescales of several factors relevant to hail growth, namely, updraft lifetime τ, time τ_a taken for hail to be advected across the updraft, and the time τ_m needed for hail growth. For single-cell storms that develop in a weakly sheared and low/moderate convective available potential energy (CAPE) environment, $\tau \ll \tau_m$, which precludes the formation of large hail. This condition implies an updraft duration of 20 min or less. Also, the updrafts in these storms are likely to be narrow, resulting in an additional limiting factor, $\tau_a < \tau_m$. By contrast, for a supercell storm, $\tau_a \geq \tau_m \leq \tau$, which favors the growth of large hail. For multicell storms, the overlap between τ_a, τ, and τ_m will determine whether hail can reach the optimum size for a given updraft velocity and liquid water content (LWC). Thus, Foote's findings point to the rationale of calculating updraft duration based on the CAPE and vertical wind shear.

Field observations and cloud-model simulations indicate that the strength of convection is largely determined by the amount of CAPE, whereas the vertical wind shear determines the organization and longevity of the convective updrafts (Chisholm and Renick 1972; Marwitz 1972a,b; Knight et al. 1982b; Fankhauser and Wade 1982; Weisman and Klemp 1982; Cotton and Anthes 1989). In general, as the CAPE and vertical wind shear increase, so does the potential for organized and long-lived updrafts. The updraft in a single-cell thunderstorm typically lasts 20–30 min (Chisholm and Renick 1972; Hand and Conway 1995), whereas in a supercell thunderstorm the updraft lasts 60 min or more (Chisholm and Renick 1972). Fankhauser and Wade (1982) found that the lifetime of convective cells, defined by the duration of the 45-dB*Z* echo aloft, observed on 52 hail days in Colorado, ranged between 10 and 120 min. The average cell lifetime was 24 min. Only 2% of the cells lasted longer than 60 min; 90% lasted less than 45 min. Another radar study of midlatitude thunderstorms by Henry (1993) indicated that 83% of the single-cell storms dissipated within 30 min. By contrast, 88% of the organized storms lasted more than 30 min, and, of these, 47% lasted more than 60 min (Henry 1993).

Calculations by Knight et al. (1982a) indicate that it takes 55 min to grow a 3-cm hailstone at an LWC of 2 g m^{-3}. Increasing the LWC to 3 g m^{-3} reduces the growth time to 35 min. Three-dimensional simulations of hailstorms (Xu 1983; Nelson 1983; Foote 1984) suggest that large hailstones can grow from a 5-mm hydrometeor in 10–20 min depending on the LWC in the hail growth zone. Heymsfield (1982) showed that it takes 20–25 min to grow a 5-mm hydrometeor from a cloud droplet. Because a much smaller embryo of 0.03 cm is used in HAILCAST, the growth times for large hail are expected to lie in the range calculated by Knight et al. (1982a).

In HAILCAST, the updraft duration is estimated using

TABLE 1. Mean instability and vertical wind shear parameters for different storm types, and the corresponding updraft durations determined from radar observations and numerical model simulations.

Observations	CAPE (m^{-2} s^{-2})	Wind shear (10^{-3} s^{-1})	CAPE × SHEAR (m^2 s^{-3})	Cell/updraft duration (min)
Alberta [Chisholm and Renick (1972)]				
Single cell	~400	~1.0[a]	0.40	20
Multicell	~850	~4.3[a]	3.70	20–40
Supercell	~1400	~5.5[a]	7.70	>60
Colorado [Fankhauser and Wade (1982), Knight et al. (1982b)]				
Weak storms	400	2.5	1.00	~15
Multicellular storms	700	2.9	2.03	~25
Long-lived unicellular storms	900	5.0	4.50	>50
Southern plains [Weisman and Klemp (1982)]				
Single cell	2200	~0.1[b]	0.22	30
Multicell	2200	~1.8[b]	3.91	50
Supercell	2200	~3.0[b]	6.60	>120
Switzerland [Houze et al. (1993)]				
Low-energy and low-shear storms	~870	~2.7[c]	2.37	~55
High-energy and high-shear storms	~1770	~3.9[c]	6.84	~100

[a] Vertical wind shear calculated from Fig. 3 in Chisholm and Renick (1972).
[b] Vertical wind shear calculated from Fig. 8 in Weisman and Klemp (1982).
[c] Vertical wind shear calculated between the surface and 500 hPa.

the products of CAPE × SHEAR (Brimelow 1999), where CAPE denotes the observed surface-based convective available potential energy and ''SHEAR'' denotes the magnitude of the mean vertical shear of the observed winds recorded between 1.5 and 6.0 km MSL (Penhold, Alberta, 905 m MSL). The rationale is to account for the combined effects of buoyancy and vertical wind shear on the updraft duration, with larger products indicating an increased potential for long-lived updrafts (Brimelow 1999).

To examine this method of estimating updraft duration, we calculated mean CAPE and SHEAR for different storm types and compared these data with the corresponding updraft durations determined from radar observations (Chisholm and Renick 1972; Knight et al. 1982b; Fankhauser and Wade 1982; Houze 1993) and model simulations (Weisman and Klemp 1982). Although radar echoes are not always collocated with updrafts in convective cells, we believe that the criteria used by Fankhauser and Wade (1982) would single out those convective cells in their developing and mature stages. The updraft durations from Weisman and Klemp's (1982) model simulations were obtained using a threshold of 10 m s^{-1} (see their Fig. 3).

The data in Table 1 indicate an increasing trend in values of CAPE × SHEAR as the storm severity and updraft duration increase. In particular, values of CAPE × SHEAR for single-cell thunderstorms, having updraft duration of about 20 min, are less than 1 m^2 s^{-3}. By comparison, values of CAPE × SHEAR for the supercell thunderstorms, having updraft duration greater than 60 min, are all greater than about 5 m^2 s^{-3}. Thus, these data suggest that the product of CAPE and shear is a suitable parameter for determining the updraft duration for a wide range of convective environments.

TABLE 2. Parameterization scheme used to relate updraft duration to the CAPE and vertical wind shear.

CAPE × SHEAR (m^2 s^{-3})	≤1	2	3	≥5
Updraft duration (min)	20	35	45	60

Based on both the observational and modeling data presented in Table 1, we adopted the parameterization scheme of Brimelow (1999) that relates the updraft duration to CAPE × SHEAR (Table 2). The lower and upper limits of updraft duration were 20 and 60 min, respectively. For values of CAPE × SHEAR that lie between the integer values listed in Table 2, interpolation was used to determine the corresponding updraft duration.

It should be stressed that the assumptions needed for ''estimating'' updraft duration stem from the difficulty of linking a steady-state model component with a time-dependent model component. If one were to use a time-dependent 3D cloud model, then the hailstone trajectories could be estimated and the residence time of the hailstone within the updraft would be solved naturally. This makes time-dependent cloud modeling an attractive option, because fewer model assumptions are required. Of course, other complications would arise such as choosing the appropriate trajectory that would maximize the hail size.

4. Case study of 11 July 1985

a. Background

In this section, we describe the model-derived updraft profile and hail growth time history for a severe-hail day observed in central Alberta on 11 July 1985. Smith

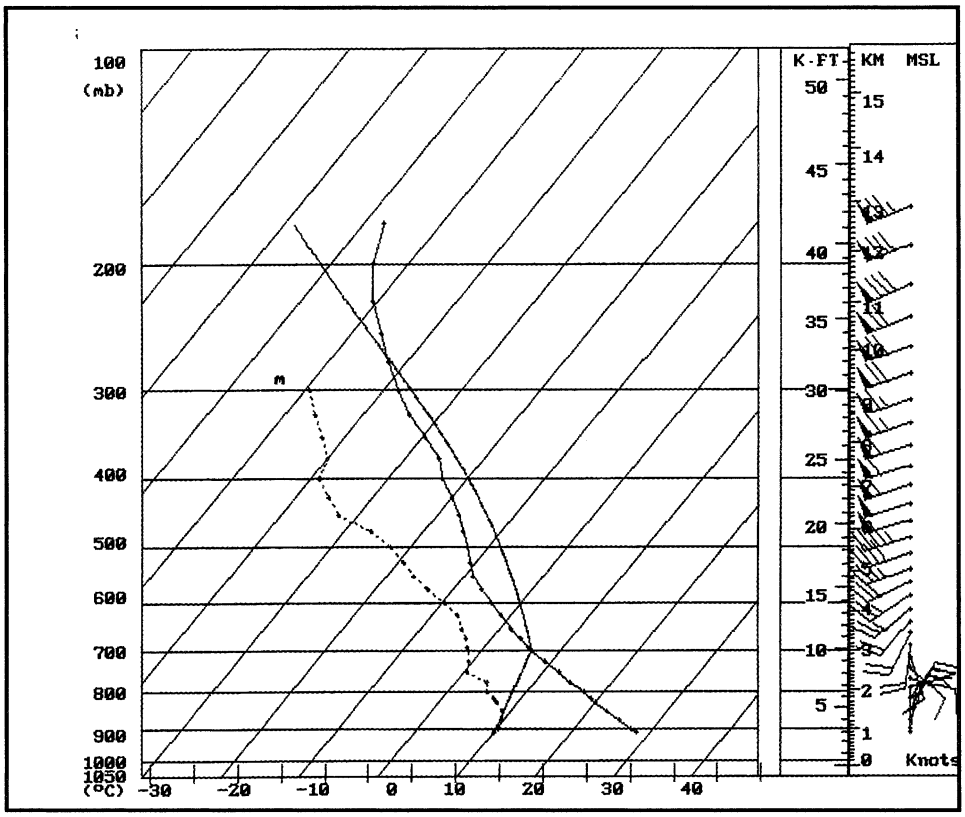

FIG. 2. Upper-air sounding released from Penhold at 1715 LT on 11 Jul 1985 plotted on a skew *T*–log*p* diagram. The dashed line represents the dewpoint profile, the solid line is the environmental temperature, and the curved solid line is the pseudoadiabat (based on the observed surface temperature and dewpoint).

and Yau (1993a) conducted a detailed investigation of the events on this day.

After 1600 LT, several severe thunderstorms developed over the foothills north of Rocky Mountain House and moved eastward onto the prairies. For several hours, the maximum reflectivities of the most intense storms were observed to exceed 60 dBZ. A total of 228 hail reports were received within the northern half of the Alberta Hail Project area, of which 33 were severe. The largest reported hail was classified as golfball (3.3–5.2 cm in diameter), with the longest observed hailswath estimated to be over 200 km long.

The most prominent features of the 1715 LT upper-air sounding released from Penhold were the relatively high buoyant energy and strongly sheared wind profile (Fig. 2). Easterly to north-easterly winds of 5 m s^{-1} in the boundary layer veered to west-southwesterly winds of 40 m s^{-1} near the tropopause. The surface-based CAPE of 756 J kg^{-1} and strong vertical wind shear in the lowest 6 km AGL (6.5×10^{-3} s^{-1}) indicated the potential for strong and sustained deep convection.

b. Model output

Figure 3 shows the model-derived profiles of updraft velocity and LWC. The updraft increased from 4 m s^{-1} at the cloud base (near 7°C) to a maximum of 26.9 m s^{-1} near −23°C (Fig. 3a). This is 70% of the maximum buoyancy-derived value of 38.8 m s^{-1} [determined using $W_{max} = (2\text{CAPE})^{0.5}$]. The forecast cloud-top temperature was −49.6°C (9700 m AGL). The LWC reached its maximum value of 3.5 g m^{-3} at −26.4°C (approximately 7200 m AGL). This closely corresponds to the height of the forecast maximum updraft velocity.

Figure 4 depicts the simulated growth history of a hailstone. A 300-μm droplet introduced into the updraft at the cloud base freezes after passing through the −8°C level and enters the dry growth regime. The hailstone remains in the dry growth regime and continues to rise rapidly through the supercooled region of the cloud. When it reaches the −40°C level, after 9 min, the hailstone is 0.2 cm in diameter, and while above this level it grows very slowly by accreting ice crystals. After 46 min, the hailstone has grown sufficiently to descend below the −40°C level and reenters the mixed-phase region of the cloud. Doing so initiates a period of rapid growth between 46 and 57 min, because the stone is now 1.3 cm in diameter and is located in a region having a high LWC. During its descent, the hailstone encounters strong updrafts and is prevented from falling prematurely from the cloud. This allows the hailstone to grow substantially from 1.3 to 5.0 cm in diameter during

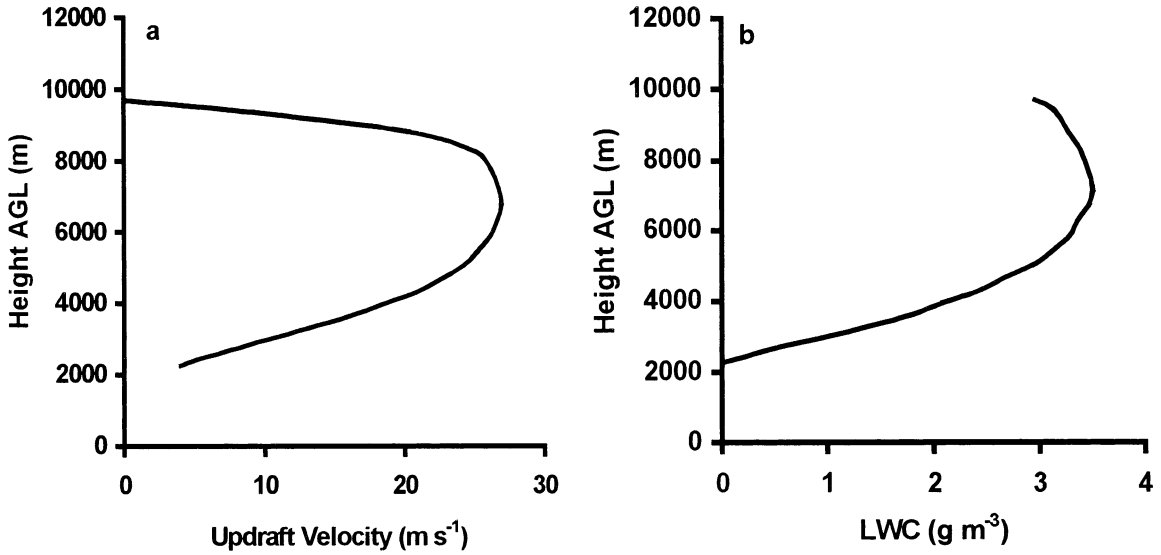

FIG. 3. Model-derived profiles of (a) updraft velocity and (b) LWC for 11 Jul 1985.

its 14-min passage through the supercooled region of the cloud. As the hailstone accretes water during its descent, the latent heat of freezing causes the hailstone's surface temperature to rise steadily. It enters the wet growth regime after 58 min at an in-cloud temperature of −12.6°C. Thereafter, the shedding of excess water from the hailstone's surface slows the rate of growth. The maximum diameter of 5.0 cm is attained after 60 min and decreases thereafter because of melting below the freezing level. When the hailstone is near 3590 m AGL (−1.2°C), the updraft collapses, and the hailstone spends less than 3 min below the freezing level before reaching the ground after 62 min with a final diameter of 4.1 cm (terminal velocity 28.5 m s^{-1}).

c. Sensitivity experiments

We now investigate the sensitivity of the model-derived updraft profile and hail growth to changes in selected cloud and microphysical parameters. The control for the sensitivity experiments is based on the severe hailstorm sounding of 11 July 1985. The forecast cloud variables of interest are W_0 (updraft velocity at cloud base), $W_{\max}$ (maximum updraft velocity), $T_{w\max}$ (temperature at the altitude of $W_{\max}$), and Z_{top} (cloud-top height). Two parameters related to hail growth are also discussed: D_f (hail diameter on the ground) and τ_f (time when hailstone reaches the ground).

Observations of hailstorms in Alberta (Chisholm 1973) and the High Plains (Auer and Marwitz 1972) show that W_0 typically varies between 2 and 8 m s^{-1}. Experiments C1–C3 (Table 3) show that $W_{\max}$ and Z_{top} both increase slightly as W_0 is increased from 2 to 6 m s^{-1}. These changes have a minimal effect on D_f, but there is an increase in τ_f. This increase in τ_f can be attributed to the modeled hailstone spending more time aloft on account of the stronger updrafts. The same trends in D_f and τ_f are evident for a 0.1-cm embryo (C4–C6). No hail is produced in experiment C4 because the cloud-base updraft velocity of 2 m s^{-1} is not sufficient to suspend a 1-mm droplet having a terminal velocity of approximately 4 m s^{-1}. As a result, the droplet falls from the cloud and the model run is terminated.

Next we investigate the sensitivity of the modeled cloud and hail to the amount of entrainment. Betts's (1982b) entrainment parameter β represents the percentage of environmental air that mixes with the updraft. Experiments C7–C10 show that reducing β from 10% to 0% increases $W_{\max}$ from 26.3 to 28.6 m s^{-1} and lowers $T_{w\max}$ from −22.6° to −30.2°C. However, the increase in $W_{\max}$ is not accompanied by an increase in D_f. This paradox can be explained by considering the results from experiments H1–H5 (Table 4). These experiments indicate that D_f is sensitive to the upper limit of 60 min placed on τ if the modeled cloud has a strong updraft (>25 m s^{-1}) and if D_0 is smaller than 0.03 cm. Under these conditions, the modeled hailstone is advected rapidly above −40°C and becomes trapped in the glaciated portion of the cloud. The final hail size is now primarily determined by the hailstone's position with respect to the −40°C level when the updraft collapses. Should the updraft collapse before the hailstone reenters the supercooled region of the cloud, the hailstone rapidly descends through the hail growth zone and is consequently much smaller when it reaches the ground. These results are consistent with the findings of English (1973). She found that, in modeled storms with weak to moderate updrafts, a wide range of hail embryo sizes (0.03–0.08 cm) could produce the same maximum hail size. However, for storms with updrafts greater than 25 m s^{-1}, the largest hail was only modeled for embryos greater than 0.08 cm in diameter. Experiments using a 0.01-cm

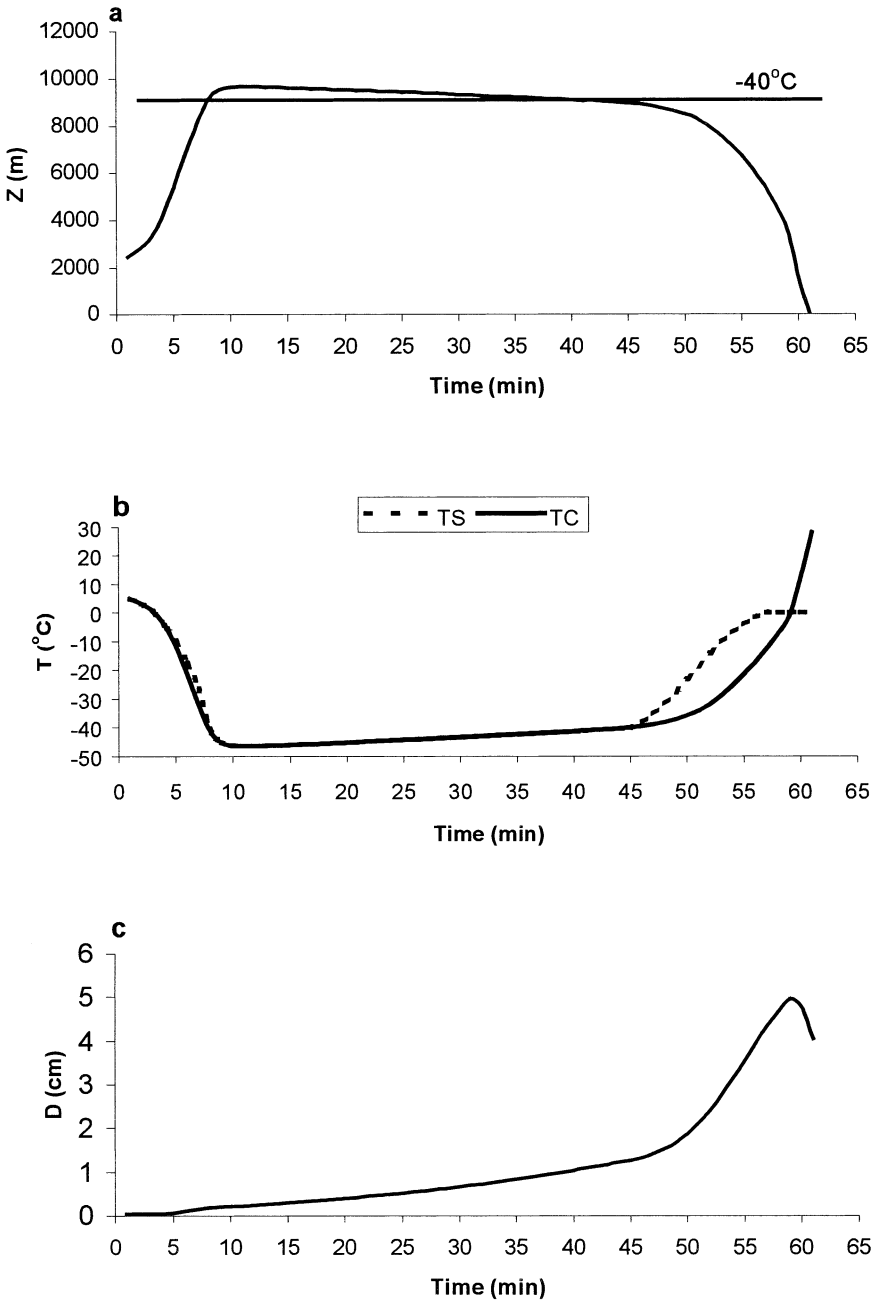

FIG. 4. Growth time history of a hailstone simulated by HAILCAST for 11 Jul 1985. Depicted are (a) height (Z), (b) in-cloud (TC) and hailstone temperature (TS), and (c) diameter (D).

hail embryo (C11–C14) show that D_f increases from 3.7 to 4.3 cm as β is reduced from 10% to 0%. For both the 0.03- and 0.1-cm embryos, τ_f increases slightly as β is reduced from 10% to 0%. As before, the longer times stem from the increase in residence time of the hailstone in the glaciated portion of the cloud as $W_{\max}$ increases.

We now discuss the sensitivity experiments for selected microphysical parameters. All the sensitivity experiments were run using the control updraft profile and in-cloud properties. Experiments H1–H5 (Table 4) indicate that D_f is not sensitive to the initial embryo diameter, provided that D_0 is at least 0.03 cm. The time τ_f, to reach the ground however, decreases from 61.9 to 50.9 min, as D_0 is increased from 0.03 and 0.1 cm. This is due to the lower trajectory and larger cross-sectional area of the hailstone forming on the larger embryo.

In experiments H6–H13, the temperature T_0 at which the hail embryo freezes was varied between $-5°$ and

TABLE 3. Sensitivity experiments (C1–C6) showing the effect of changing the updraft velocity at cloud base (W_0) on W_{max} (maximum updraft velocity), T_{wmax} (temperature at the updraft maximum), Z_{top} (cloud-top height, height at which the updraft velocity is zero), D_f (hail diameter on the ground), and τ_f (time at which hailstone reaches the ground). Experiments C7–C14 show the effect of changing the percentage of environmental air (β) entrained into the updraft. Also listed is the size of the initial hail embryo introduced at cloud base (D_0). Control values are highlighted in boldface.

Expt	W_0 (m s^{-1})	D_0 (cm)	β (%)	W_{max} (m s^{-1})	T_{wmax} (°C)	Z_{top} (m)	D_f (cm)	τ_f (min)
C1	2	0.03	7.5	26.7	−22.5	10 580	4.0	62.2
C2	**4**	**0.03**	**7.5**	**26.9**	**−22.7**	**10 640**	**4.1**	**61.9**
C3	6	0.03	7.5	27.3	−22.3	10 790	4.0	62.5
C4	2	0.1	7.5	26.7	−22.5	10 580	—	—
C5	4	0.1	7.5	26.9	−22.7	10 640	3.9	50.9
C6	6	0.1	7.5	27.3	−22.3	10 790	3.9	51.7
C7	4	0.03	0.0	28.6	−30.2	11 200	2.3	65.0
C8	4	0.03	5.0	27.2	−23.0	10 860	3.9	62.8
C9	**4**	**0.03**	**7.5**	**26.9**	**−22.7**	**10 640**	**4.1**	**61.9**
C10	4	0.03	10.0	26.3	−22.6	10 370	3.7	58.3
C11	4	0.1	0.0	28.6	−30.2	11 200	4.3	59.1
C12	4	0.1	5.0	27.2	−23.0	10 860	4.0	53.1
C13	4	0.1	7.5	26.9	−22.7	10 640	3.9	50.9
C14	4	0.1	10.0	26.3	−22.6	10 370	3.7	46.8

TABLE 4. Sensitivity experiments showing the effect of changing the initial hail embryo diameter (D_0), the embryo freezing temperature (T_0), the density of accreted ice (ρ_i), and the updraft duration (τ) on D_f and τ_f. Control values are highlighted in boldface.

Expt	D_0 (cm)	T_0 (°C)	ρ_i (g cm^{-3})	τ (min)	D_f (cm)	τ_f (min)
H1	0.01	−8	0.90	60	1.5	66.5
H2	**0.03**	**−8**	**0.90**	**60**	**4.1**	**61.9**
H3	0.05	−8	0.90	60	3.9	58.0
H5	0.10	−8	0.90	60	3.9	50.9
H6	0.03	−5	0.90	60	4.1	61.8
H7	**0.03**	**−8**	**0.90**	**60**	**4.1**	**61.9**
H8	0.03	−15	0.90	60	4.1	61.9
H9	0.03	−30	0.90	60	4.1	62.1
H10	0.1	−5	0.90	60	3.9	50.9
H11	0.1	−8	0.90	60	3.9	50.9
H12	0.1	−15	0.90	60	3.9	51.0
H13	0.1	−30	0.90	60	3.9	51.3
H14	**0.03**	**−8**	**0.90**	**60**	**4.1**	**61.9**
H15	0.03	−8	0.85	60	4.3	61.8
H16	0.03	−8	0.80	60	4.6	61.8
H17	0.1	−8	0.90	60	3.9	50.9
H18	0.1	−8	0.85	60	4.1	51.3
H19	0.1	−8	0.80	60	4.4	51.6
H20	0.03	−8	0.90	50	1.7	55.9
H21	0.03	−8	0.90	55	3.0	59.0
H22	**0.03**	**−8**	**0.90**	**60**	**4.1**	**61.9**
H23	0.03	−8	0.90	65	4.1	61.9
H25	0.1	−8	0.90	40	2.0	45.4
H26	0.1	−8	0.90	45	3.4	48.4
H27	0.1	−8	0.90	50	4.0	50.8
H28	0.1	−8	0.90	55	3.9	50.9

−30°C. Decreasing T_0 had a negligible impact on D_f for both the 0.03- and 0.1-cm embryos. This is likely due to the hail embryo ascending rapidly through the cloud, and any changes in growth rate resulting from a decrease in the embryo's density upon freezing would not have sufficient time to significantly influence D_f. Lowering T_0 slightly increased τ_f.

Ziegler et al. (1983) suggested that, under certain conditions, low-density ice accretion may be important for the growth of large hail. In experiments H14–H19, we varied the ice density ρ_i between 0.8 and 0.9 g cm^{-3}. This range was based on the observed density of natural hailstones provided by English (1973). For a 0.03-cm embryo, reducing ρ_i from 0.9 to 0.8 g cm^{-3} increases D_f from 4.1 to 4.6 cm. Decreasing ρ_i had little effect on τ_f. Experiments using a 0.1-cm embryo (H17–H19) show a similar trend. These findings are consistent with those made in similar experiments conducted by English (1973) and Ziegler et al. (1983).

Experiments H20–H28 examine the sensitivity of the modeled hail growth to the updraft duration τ. For a 0.03-cm embryo, decreasing the updraft duration from 60 to 50 min decreases D_f from 4.1 to 1.7 cm. This decrease in hail size is consistent with the time (approximately 10 min) required for a hailstone to grow from 2 to 4 cm at an LWC of 3.0 g m^{-3}. Similarly, for a 0.01-cm embryo (H25–H28), D_f decreases from 3.9 to 2.0 cm, when τ is decreased from 50 to 40 min. Extending τ beyond τ_f has no effect on the final hail size for both embryo sizes. According to our method of calculating τ (section 3c), a 10-min (~20%) decrease in τ is equivalent to decreasing the CAPE (or vertical wind shear) by 40%, that is, from 756 to 460 J kg^{-1} (or 6.5×10^{-3} to 4.0×10^{-3} s^{-1}). A CAPE of 460 J kg^{-1} translates into an updraft velocity of approximately 15 m s^{-1} (after allowing for entrainment and water loading), which is capable of suspending a 1.5-cm hailstone aloft. Thus, the forecast decrease and hail size associated with the decrease in updraft duration shown in experiments H20–H28 seem reasonable.

5. Hail forecast evaluation

In this section, forecasts of maximum hail size determined using the HAILCAST model and Renick and Maxwell's (1977) nomogram (referred to as RAM) are evaluated against observations of maximum hail size within the Alberta Hail Project area. Each model forecast hail size (on the ground) was placed in a hail-size category according to the criteria outlined in section 2. The maximum updraft velocity data required to determine the hail size category using RAM (Fig. 1) were obtained from the one-dimensional steady-state cloud model.

To objectively assess the model and nomogram hail forecasts, we calculated several skill scores derived from 2×2 contingency tables; Marzban and Stumpf (1998) provide a summary of the skill scores derived from a 2×2 contingency table. An example of a contingency table used in our research is shown in Table 5. A hit was noted when hail was forecast and hail was observed between 1415 and 2015 LT and within 100 km of Pen-

TABLE 5. Example of a 2 × 2 contingency table used to derive skill scores for the objective evaluation of the HAILCAST and RAM hail forecasts for 62 hail days.

		Forecast	
		Hail	No hail
Observed	Hail	53 (hit)	9 (miss)
	No hail	19 (false alarm)	79 (null forecast)

hold; a false alarm was noted when hail was forecast but none was observed; a miss was recorded when no hail was forecast but hail was observed; and, finally, a null forecast was recorded when no hail was forecast and none was observed. The following skill scores are compared: probability of detection (POD), false-alarm ratio (FAR), and Heidke skill score (HSS). HSS is a popular skill score for the verification of rare-event forecasts and measures the true skill of a forecast because it takes all values in the contingency table into account (Doswell et al. 1990). The HSS varies between −1 for absolutely no forecast skill and 1 for a perfect forecast.

Both HAILCAST and RAM showed skill when forecasting the occurrence of hail. RAM scored a POD of 0.90, versus 0.85 for HAILCAST (Fig. 5). This equates to correctly forecasting 56 and 53 of the 62 hail days in the dataset, respectively. RAM, however, scored a markedly higher FAR of 0.33 (26 false alarms), versus 0.26 for HAILCAST (19 false alarms). A possible explanation for the relatively high number of false alarms will be discussed in section 6. Both techniques displayed good overall skill when forecasting the occurrence of hail. However, the model scored an HSS of 0.64, which was higher than that scored by RAM (HSS = 0.56).

For the hail-size forecasts, the model was appreciably more accurate than RAM when forecasting the hail-size category (Table 6). HAILCAST correctly forecast the hail-size category on 39% of the 62 hail days, versus only 27% for RAM. Moreover, 81% of the HAILCAST forecasts were within one size category; this percentage was noticeably higher than for RAM (74%). Both HAILCAST and RAM tended to underestimate the hail-size category, with 38% and 54% of the forecasts being one or more categories too small, respectively. HAILCAST forecast hail one or more categories too large for 23% of the forecasts, versus 19% for RAM. Both techniques rarely overestimated the hail size by more than two categories.

TABLE 6. Hail-size forecast performance of HAILCAST and RAM for 62 hail days and 20 severe hail days between 1983 and 1985.

	Hail days		Severe-hail days	
Hail-size category	HAILCAST (%)	RAM (%)	HAILCAST (%)	RAM (%)
Correct	39	27	40	30
Within one	81	74	95	70
One too small	27	31	35	35
Two or more too small	11	23	5	25
One too large	15	16	20	5
Two or more too large	8	3	0	5

To evaluate the forecast skill more thoroughly, it is advantageous to distinguish between severe- and non-severe-hail days, based on hail size. Days with reported hail diameters of walnut or larger (i.e., maximum hailstone diameter greater than 2.0 cm) were classified as severe-hail days. This classification by maximum size was motivated by the work of Smith et al. (1998).

Figure 6 shows that HAILCAST displayed significant skill when forecasting the occurrence of severe hail, with a POD of 0.90, as compared with only 0.65 for

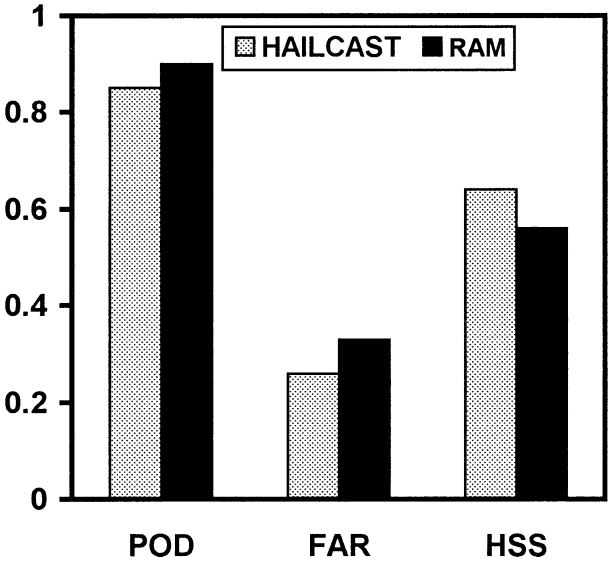

FIG. 5. Summary of skill scores for HAILCAST and RAM for 62 hail days between 1983 and 1985.

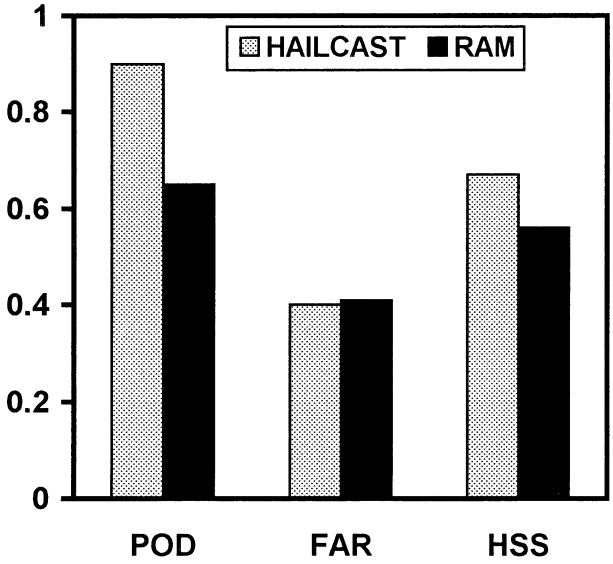

FIG. 6. Summary of skill scores for HAILCAST and RAM for 20 severe-hail days between 1983 and 1985.

RAM. These values equate to correctly forecasting 18 and 13 of the 20 severe-hail days, respectively. On days when severe hail was observed but not forecast, both techniques forecast at least pea-sized hail. HAILCAST missed two severe-hail days, and on both of these days the model forecast grape-sized hail, with forecast diameters of 2.0 and 1.8 cm, respectively. HAILCAST, therefore, did anticipate the formation of relatively large hail, with both the forecast diameters being very close to the severe-hail threshold. By comparison, RAM forecast grape-sized hail for two of the seven misses and pea-sized hail on the remainder. When compared with forecasts for all days with hail (i.e., nonsevere- and severe-hail days), both RAM and HAILCAST scored relatively high false-alarm ratios. RAM scored a marginally higher FAR of 0.41 (9 false alarms) versus 0.40 (12 false alarms) for HAILCAST. Once again, HAILCAST displayed greater overall skill and scored an HSS of 0.67, as compared with 0.56 for RAM.

Table 6 indicates that HAILCAST was more accurate than RAM when forecasting the hail-size category for the severe-hail days. Forty percent of the model forecasts on severe-hail days were correct (versus 30% for RAM), and 95% were within one size category (as compared with 70% for RAM). As was the case for the nonsevere-hail days, both techniques tended to underestimate the hail-size category. Forty percent of the model forecasts were one or more categories too small, as compared with 60% for RAM. HAILCAST forecast hail two or more categories too small on only 6% of the severe-hail days, versus 25% for RAM.

The HAILCAST model has since been applied successfully to a dataset removed in both space and time from the AHP. Between 15 October 1999 and 15 March 2000, HAILCAST was used operationally to provide forecasts of maximum hail size for a hail-suppression project in Mendoza, Argentina (Brimelow et al. 2002). A representative sounding (released at 1200 LT) and subjective forecasts of the maximum surface temperature and coincident dewpoint were used as input for the model. The model predictions of maximum hail size were verified against observations made within the project area. Hail was observed on 38 of the 118 days used in the evaluation. The performance statistics were POD = 0.76, FAR = 0.29, and HSS = 0.60 (Brimelow et al. 2002).

6. Discussion of false alarms

The forecast evaluation in section 5 revealed a number of occasions on which the model and nomogram forecast hail and none was observed. To examine this tendency to overforecast hail events, 19 days were identified on which hail was forecast but not observed over the project area.

Despite sufficient moisture and convective instability, thunderstorms can be prevented from developing because of the absence of a trigger mechanism (Mueller et al. 1993). Moreover, Smith and Yau's (1993b) conceptual model for severe-weather outbreaks in Alberta highlights the need for the interaction of the synoptic and mesoscale environments to trigger severe convection. They found that 94% of all severe-hail days were associated with an upper-air (500 hPa) trough upwind of Alberta. By contrast, 71% of no-hail days had an upper-air ridge over Alberta. The reduced wind shear and subsidence aloft observed on such occasions often result in no deep convection or in short-lived airmass thunderstorms that rarely produce large hail. On 17 of the 19 days when HAILCAST incorrectly forecast hail, the upper-air circulation over the project area at 1800 LT was dominated by a ridge and only towering cumulus or cumulus clouds were observed. On the remaining two days, when a trough was located upwind of Alberta, thunderstorms developed over the foothills but no hail was reported within the AHP area [for details, see Brimelow (1999)]. Neglecting model output on days when a ridge dominated the upper-air circulation over the AHP area reduces the number of false alarms of hail to 2 (from 19), and this, in turn, significantly reduces the FAR from 0.26 to 0.04. Applying the upper-ridge criteria for days when severe hail was forecast and not observed reduces the false alarms of severe hail to 8 (from 12), with a resultant decrease in the FAR from 0.40 to 0.31.

The above discussion illustrates that HAILCAST calculates the maximum hail size according to the surface-based convective instability and is not always capable of determining whether factors will be present to inhibit or to prevent this instability from being released. For example, on days when a weak capping lid (<-15 J kg^{-1}) is present, the user is unable to specify if sufficient lift will be present to lift a parcel from the LCL to the level of free convection. This is particularly important for days on which large CAPE is present above the lid but a lifting mechanism is either absent or is too weak to initiate convection. On these days, using an updraft velocity of 4 m s^{-1} at the LCL may not be appropriate, and the model may incorrectly predict hail. The model forecast can still be of value, however, because it will alert the forecaster to the threat of hail should the capping lid be removed.

Several studies have underscored the value of coupling model forecast soundings and real-time surface data to forecast thunderstorm initiation (Mueller et al. 1993; Hart et al. 1998). Following the success of these projects, we envisage that HAILCAST will eventually be run using a combination of high spatial and temporal forecast NWP soundings that correspond in space and time with surface observations of temperature, moisture, and wind. The surface data will be used to modify the lowest levels of the virtual sounding; the model data will be retained above this level. Surface conditions at model grid points lying between observation stations will be determined using interpolation. Next, several instability and convection inhibition parameters will be

calculated by lifting the most unstable parcel in the lowest 1.5–2 km above the surface. An objective decision tree [similar to that of Mills and Colquhoun (1998)] will then be applied at each grid point using the instability and convection inhibition parameters. HAILCAST will then be run at those locations for which conditions are favorable for the initiation of deep convection. The observed surface winds could also potentially be used to calculate the low-level convergence and to identify areas in which lifting is strong enough to initiate convection. In this way, hourly forecasts of hail size, in addition to a number of other model-derived parameters, could be made over a large area. We recently employed a similar version of the aforementioned technique to issue real-time maximum-hail-size forecasts for the Alberta Hail Suppression Project. Preliminary results suggest that this technique shows significantly more forecast skill than forecasts based on a modified 1200 UTC sounding located some 150 km north of the project area.

7. Conclusions

This paper addresses the problem of predicting maximum hail size on the ground by employing a one-dimensional steady-state cloud model, coupled with a time-dependent hail growth model (HAILCAST). Model forecasts were based on the 1715 LT proximity soundings released from the center of the AHP area and representative surface temperatures and coincident dewpoints recorded by a mesonetwork.

To evaluate HAILCAST objectively, the model forecasts of maximum hail size were verified against reports of maximum hail size gathered from a high-density observation network within the AHP area for 160 days between 1983 and 1985. The performance of HAILCAST was also compared with that of a nomogram (RAM) developed by Renick and Maxwell (1977) to forecast maximum hail size in Alberta. The maximum updraft velocity data required to determine the hail-size category using RAM were obtained from the cloud model.

HAILCAST displayed greater overall skill than RAM when forecasting the occurrence of hail and scored a Heidke skill score of 0.64, as compared with 0.56 for RAM. The model performed especially well on severe-hail days and scored an HSS of 0.67, versus only 0.56 for RAM. HAILCAST was more accurate than RAM when forecasting the hail-size category, with 81% of the model hail forecasts within one size category, as compared with 74% for RAM. On severe-hail days, 95% of the model forecasts were correct to within one size category as compared with only 70% for RAM. Both techniques tended to overforecast the occurrence of hail. These false alarms occurred mainly when an upper ridge was present above the AHP area.

The results presented in this paper indicate that HAILCAST is a useful aid for objectively forecasting hail and is capable of distinguishing between nonsevere- and severe-hail events. HAILCAST also shows promise for predicting the occurrence and size of hail on the ground. We have also shown that forecasting hail using a coupled cloud and hail model noticeably improves the overall skill and accuracy of the forecasts over those of Renick and Maxwell's (1977) nomogram, especially on severe-hail days. Furthermore, HAILCAST has also been applied successfully to a dataset removed in both space and time from the AHP (Brimelow et al. 2002).

Short-range forecasts of severe thunderstorms are critically dependent on the availability of a sounding representative of the expected thunderstorm environment. One means of addressing the problem of obtaining representative soundings in advance would be to use a regional numerical weather prediction model to provide prognostic soundings at each grid point within the model's domain. A decision tree similar to that developed by Mills and Colquhoun (1998) could be applied at each grid point to determine whether conditions are favorable for thunderstorm formation. HAILCAST would then be run using the virtual sounding data at grid points at which thunderstorms are expected. Also, in light of the uncertainty of the NWP model input data, the hail model should be run using a quasi–Monte Carlo or similar ensemble approach as proposed by Brooks et al. (1992, 1993). This approach would allow forecasters to identify quickly and easily those areas most at risk for hail and to provide an estimate of the maximum hail size.

Acknowledgments. The authors appreciate the thoughtful comments of anonymous reviewers that helped to clarify the model description and its sensitivity. Dr. Geoff Strong provided the Alberta Hail Project sounding data. The research was supported by grants from the Natural Sciences and Engineering Research Council (NSERC) and the Canadian Foundation for Climate and Atmospheric Sciences (CFCAS).

REFERENCES

Admirat, P., G. G. Goyer, L. Wojtiw, E. A. Carte, D. Roos, and E. P. Lozowski, 1985: A comparative study of hail in Switzerland, Canada and South Africa. *J. Climatol.*, **5,** 35–51.

Al-Jumily, K. J., R. C. Charlton, and R. G. Humphries, 1991: Identification of rain and hail with circular polarization radar. *J. Appl. Meteor.,* **30,** 1075–1087.

Anthes, R. A., 1977: A cumulus parameterization scheme utilizing a one-dimensional cloud model. *Mon. Wea. Rev.,* **105,** 270–286.

Auer, A. H., Jr., and J. D. Marwitz, 1972: Hail in the vicinity of organized updrafts. *J. Appl. Meteor.,* **11,** 748–751.

Betts, A. K., 1982a: Cloud thermodynamics models in saturation point coordinates. *J. Atmos. Sci.,* **39,** 2182–2191.

——, 1982b: Saturation point analysis of moist convective overturning. *J. Atmos. Sci.,* **39,** 1484–1505.

Bluestein, H. B., E. W. McCaul Jr., G. P. Byrd, and G. R. Woodall, 1988: Mobile sounding observations of a tornadic storm near the dryline: The Canadian, Texas storm of 7 May 1986. *Mon. Wea. Rev.,* **116,** 1790–1804.

Blyth, A. M., M. Alan, W. A. Cooper, and J. B. Jensen, 1988: A study of the source of entrained air in Montana cumuli. *J. Atmos. Sci.,* **45,** 3944–3964.

Boatman, J. F., and A. H. Auer Jr., 1983: The role of cloud top entrainment in cumulus clouds. *J. Atmos. Sci.,* **40,** 1517–1534.

Brimelow, J. C., 1999: Numerical modelling of hailstone growth in Alberta storms. M.S. thesis, Dept. of Earth and Atmospheric Sciences, University of Alberta, 153 pp.
——, T. W. Krauss, and G. W. Reuter, 2002: Operational forecasts of maximum hailstone diameter in Mendoza, Argentina. *J. Wea. Mod.,* **34,** 8–17.
Brooks, H. E., C. A. Doswell III, and R. A. Maddox, 1992: On the use of mesoscale and cloud-scale models in operational forecasting. *Wea. Forecasting,* **7,** 120–132.
——, ——, and L. J. Wicker, 1993: STORMTIPE: A forecasting experiment using a three-dimensional cloud model. *Wea. Forecasting,* **8,** 352–363.
——, ——, and J. Cooper, 1994: On the environments of tornadic and nontornadic mesocyclones. *Wea. Forecasting,* **9,** 606–618.
Chisholm, A. J., 1973: Part I: Radar case studies and airflow models. *Alberta Hailstorms, Meteor. Monogr.,* No. 36, Amer. Meteor. Soc., 1–36.
——, and J. H. Renick, 1972: The kinematics of multi-cell and supercell Alberta hailstorms. Research Council of Alberta Hail Studies Rep. 72-2, 24–31.
Clark, T. L., 1982: Cloud modeling in three spatial dimensions. *Case Studies of the National Hail Research Experiment,* C. A. Knight and P. Squires, Eds., Hailstorms of the Central High Plains, Vol. 2, Colorado Assoc. Universities Press, 225–247.
Colman, B. R., 1990a: Thunderstorms above frontal surfaces in environments without positive CAPE. Part I: A climatology. *Mon. Wea. Rev.,* **118,** 1103–1122.
——, 1990b: Thunderstorms above frontal surfaces in environments without positive CAPE. Part II: Organization and instability mechanisms. *Mon. Wea. Rev.,* **118,** 1123–1144.
Cotton, W. R., and A. A. Anthes, 1989: *Storm and Cloud Dynamics.* Academic Press, 883 pp.
Deibert, R. J., 1984: An overview of weather modification activities in Alberta. *J. Wea. Mod.,* **16,** 66–72.
Dennis, A. S., and D. J. Musil, 1973: Calculations of hailstorm growth and trajectories in a simple cloud model. *J. Atmos. Sci.,* **30,** 278–288.
Doswell, C. A., III, J. T. Schaefer, D. W. McCann, T. W. Schlatter, and H. B. Wobus, 1982: Thermodynamic analysis procedures at the National Severe Storms Forecast Center. Preprints, *Ninth Conf. on Weather Forecasting and Analysis,* Seattle, WA, Amer. Meteor. Soc., 304–309.
——, R. Davies-Jones, and D. L. Keller, 1990: On summary measures of skill in rare event forecasting based on contingency tables. *Wea. Forecasting,* **5,** 576–585.
Edwards, R., and R. L. Thompson, 1998: Nationwide comparisons of hail size with WSR-88D vertically integrated liquid water and derived thermodynamic sounding data. *Wea. Forecasting,* **13,** 277–285.
English, M., 1973: Part II: Growth of large hail in the storm. *Alberta Hailstorms, Meteor. Mongor.,* No. 36, Amer. Meteor. Soc., 37–98.
Fankhauser, J. C., and C. Wade, 1982: The environment of the storms. *Case Studies of the National Hail Research Experiment,* C. A. Knight and P. Squires, Eds., Hailstorms of the Central High Plains, Vol. 1, Colorado Assoc. Universities Press, 5–33.
Farley, R. D., 1987: Numerical modeling of hailstorms and hailstone growth. Part III: Simulation of an Alberta hailstorm—natural and seeded cases. *J. Climate Appl. Meteor.,* **26,** 789–812.
Fawbush, E. J., and R. C. Miller, 1953: A method of forecasting hailstone size at the earth's surface. *Bull. Amer. Meteor. Soc.,* **34,** 235–244.
Foote, G. B., 1984: A study of hail growth utilizing observed storm conditions. *J. Climate Appl. Meteor.,* **23,** 84–101.
Foster, D. S., and F. C. Bates, 1956: A hail size forecasting technique. *Bull. Amer. Meteor. Soc.,* **37,** 135–141.
Hand, W. H., and B. J. Conway, 1995: An object-oriented approach to nowcasting showers. *Wea. Forecasting,* **10,** 327–341.
Hart, R. E., G. S. Forbes, and R. H. Grumm, 1998: The use of hourly model-generated soundings to forecast mesoscale phenomena. Part I: Initial assessment in forecasting warm-season phenomena. *Wea. Forecasting,* **13,** 1165–1185.
Henry, S. G., 1993: Analysis of thunderstorm lifetime as a function of size and intensity. Preprints, *26th Conf. on Radar Meteorology,* Norman, OK, Amer. Meteor. Soc., 138–140.
Heymsfield, A. J., 1982: A comparative study of the rates of development of potential graupel and hail embryos in High Plains storms. *J. Atmos. Sci.,* **39,** 2867–2897.
Houze, R. A., Jr., W. Schmid, R. G. Fovell, and H. H. Schiesser, 1993: Hailstorms in Switzerland: Left movers, right movers, and false hooks. *Mon. Wea. Rev.,* **121,** 3345–3370.
Knight, C. A., J. L. Miller, N. C. Knight, and D. Breed, 1982a: The 22 June 1976 case study: Precipitation formation. *Case Studies of the National Hail Research Experiment,* C. A. Knight and P. Squires, Eds., Hailstorms of the Cental High Plains, Vol. 2, Colorado Assoc. Universities Press, 61–89.
——, P. Smith, and C. Wade, 1982b: Storm types and some radar reflectivity characteristics. *Case Studies of the National Hail Research Experiment,* C. A. Knight and P. Squires, Eds., Hailstorms of the Cental High Plains, Vol. 1, Colorado Assoc. Universities Press, 81–93.
Kubesh, R. J., D. J. Musil, R. D. Farley, and H. D. Orville, 1988: The 1 August 1981 CCOPE storm: Observations and modeling results. *J. Appl. Meteor.,* **27,** 216–243.
Leftwich, P. W., 1984: Operational experiments in prediction of maximum expected hailstone diameter. Preprints, *10th Conf. on Weather Forecasting and Analysis,* Clearwater Beach, FL, Amer. Meteor. Soc., 525–528.
Macklin, W. C., 1977: The characteristics of natural hailstones and their interpretation. *Hail: A Review of Hail Science and Hail Suppression, Meteor. Monogr.,* No. 38, Amer. Meteor. Soc., 65–88.
Marwitz, J. D., 1972a: The structure and motion of severe hailstorms. Part I: Supercell storms. *J. Appl. Meteor.,* **11,** 166–179.
——, 1972b: The structure and motion of severe hailstorms. Part II: Multi-cell storms. *J. Appl. Meteor.,* **11,** 180–188.
Marzban, C., and G. J. Stumpf, 1998: A neural network for damaging wind prediction. *Wea. Forecasting,* **13,** 151–163.
Matthews, D. A., and J. F. Henz, 1975: Verification of numerical model simulations of cumulus–environmental interaction in the High Plains. *Pure Appl. Geophys.,* **113,** 803–823.
Miller, L. J., J. D. Tuttle, and C. A. Knight, 1988: Airflow and hail growth in a severe northern High Plains supercell. *J. Atmos. Sci.,* **45,** 736–762.
Mills, G. A., and J. R. Colquhoun, 1998: Objective prediction of severe thunderstorm environments: Preliminary results linking a decision tree with an operational regional NWP model. *Wea. Forecasting,* **13,** 1078–1092.
Moore, J. T., and J. P. Pino, 1990: An interactive method for estimating maximum hailstone size from forecast soundings. *Wea. Forecasting,* **5,** 508–526.
Morgan, G. M., and N. G. Towery, 1975: Small-scale variability of hail and its significance for hail prevention experiments. *J. Appl. Meteor.,* **14,** 763–770.
Mueller, C. K., J. W. Wilson, and N. A. Crook, 1993: The utility of sounding and mesonet data to nowcast thunderstorm initiation. *Wea. Forecasting,* **8,** 132–146.
Musil, D. J., 1970: Computer modeling of hailstone growth in feeder clouds. *J. Atmos. Sci.,* **27,** 474–482.
Nelson, S. P., 1983: The influence of storm flow structure on hail growth. *J. Atmos. Sci.,* **40,** 1965–1983.
Orville, H. D., and F. J. Kopp, 1977: Numerical simulation of the life history of a hailstorm. *J. Atmos. Sci.,* **34,** 1596–1618.
Paluch, I. R., 1979: The entrainment mechanism in Colorado cumuli. *J. Atmos. Sci.,* **36,** 2467–2478.
Poolman, E. R., 1992: Die voorspelling van haelkorrelgroei in Suid-Afrika (The forecasting of hail growth in South Africa). M.S. thesis, Faculty of Engineering, University of Pretoria, 113 pp.
Rasmussen, R. M., and A. J. Heymsfield, 1987a: Melting and shed-

ding of graupel and hail. Part I: Model physics. *J. Atmos. Sci.,* **44,** 2754–2763.
——, and ——, 1987b: Melting and shedding of graupel and hail. Part II: Sensitivity study. *J. Atmos. Sci.,* **44,** 2764–2782.
——, and ——, 1987c: Melting and shedding of graupel and hail. Part III: Investigation into the role of shed drops as hail embryos in the 1 August CCOPE severe storm. *J. Atmos. Sci.,* **44,** 2783–2803.
Renick, J. H., and J. B. Maxwell, 1977: Forecasting hailfall in Alberta. *Hail: A Review of Hail Science and Hail Suppression, Meteor. Monogr.,* No. 38, Amer. Meteor. Soc., 145–151.
Rennó, N. O., and E. R. Williams, 1995: Quasi-Lagrangian measurements in convective boundary layer plumes and their implications for the calculation of CAPE. *Mon. Wea. Rev.,* **123,** 2733–2742.
Sanders, F., and A. J. Garrett, 1975: Application of a convective plume model to prediction of thunderstorms. *Mon. Wea. Rev.,* **103,** 874–877.
Simpson, J., and V. Wiggert, 1969: Models of precipitating cumulus towers. *Mon. Wea. Rev.,* **97,** 471–489.
Smith, S. B., and M. K. Yau, 1993a: The causes of severe convective outbreaks in Alberta. Part I. A comparison of a severe outbreak with two nonsevere events. *Mon. Wea. Rev.,* **121,** 1099–1125.
——, and ——, 1993b: The causes of severe convective outbreaks in Alberta. Part II: Conceptual model and statistical analysis. *Mon. Wea. Rev.,* **121,** 1126–1134.
——, G. W. Reuter, and M. K. Yau, 1998: The episodic occurrence of hail in central Alberta and the Highveld of South Africa. *Atmos.–Ocean,* **36,** 169–178.
Strong, G. S., 1974: Objective measurement of Alberta hailfall. M.S. thesis, Dept. of Earth and Atmospheric Sciences, University of Alberta, 182 pp.
——, and E. P. Lozowski, 1977: An Alberta study to objectively measure hailfall intensity. *Atmos.–Ocean,* **15,** 33–53.
Vali, G., and E. J. Stansbury, 1965: Time-dependant characteristics of the heterogeneous nucleation of ice. Sci. Rep. MW-41, McGill University, Montreal, QC, Canada, 31 pp.
Weisman, M. L., and J. B. Klemp, 1982: The dependence of numerically simulated convective storms on vertical wind shear and buoyancy. *Mon. Wea. Rev.,* **110,** 504–520.
Witt, A., M. D. Eilts, G. J. Stumpf, J. T. Johnson, E. D. Mitchell, and K. W. Thomas, 1998: An enhanced hail detection algorithm for the WSR-88D. *Wea. Forecasting,* **13,** 286–303.
Xu, J. L., 1983: Hail growth in a three-dimensional cloud model. *J. Atmos. Sci.,* **40,** 185–203.
Ziegler, C. L., P. S. Ray, and N. C. Knight, 1983: Hail growth in an Oklahoma multicell storm. *J. Atmos. Sci.,* **40,** 1768–1791.